Homozygous *TRPV4* loss-of-function mutation causes a severe form of distal Hereditary Motor Neuropathy (dHMN)

Michael Mario Marchetti[1], Agnes Toth-Petroczy[1], Claire Grosgogeat[1], Jose Velilla[2], Alexis H Bennett[1], Nikkola Carmichael[1], Elicia Estrella[3], Basil T. Darras[4], Brigham Genomic Medicine[1], Natasha Y Frank[1], Joel Krier[1], Rachelle Gaudet[2], Vandana A. Gupta[1*]

[1] Division of Genetics, Brigham and Women's Hospital, Harvard Medical School, Boston, MA 02115

[2] Department of Molecular and Cellular Biology, Harvard University, Cambridge, MA 02138

[3] Division of Genetics, Boston Children's Hospital, Boston, MA 02115

[4] Division of Neurology, Boston Children's Hospital, Harvard Medical School, Boston, MA 02115

* Corresponding Author

Vandana A Gupta
Division of Genetics
Department of Medicine
Brigham and Women's Hospital
Harvard Medical School
Boston, MA 02115
Email: vgupta@research.bwh.harvard.edu

Financial Disclosure

Mr. Marchetti reports no disclosures.

Dr. Toth-Petroczy reports no disclosures.

Ms. Grosgogeat reports no disclosures.

Mr. Velilla reports no disclosures.

Ms. Bennett reports no disclosures.

Ms. Carmichael reports no disclosures.

Ms. Estrella reports no disclosures.

Dr. Darras has received royalties as the author of articles regarding neuromuscular diseases for UpToDate, Inc. UpToDate does not produce healthcare-related products or services. Dr. Darras has served as consultant (ad hoc Scientific Advisory Board member) for Sarepta Inc., AveXis, Inc., BMS, Inc., Cytokinetics, Inc., Biogen, Inc., Marathon, Inc., Santhera, Inc., and Roche, Inc.; receives research support from PTC, Inc., Summit, Inc., Fibrogen, Inc., Santhera, Inc., Cyokinetics, Inc., Biogen, Inc., AveXis, Inc., Roche, Inc., the National Institutes of Health (NINDS, 5U10NS077269), the SMA Foundation, Working on Walking Foundation, and the Slaney Family Fund for SMA. Dr. Darras has no conflicts of interest regarding this manuscript.

Dr. Frank is a co-inventor of the ABCB5-related US patents assigned to Brigham and Women's Hospital, Boston, Massachusetts, and licensed to Ticeba GmbH (Heidelberg, Germany) and Rheacell GmbH & Co. KG (Heidelberg, Germany). She also serves as an Advisor to Veritas Genetics, Inc. (Danvers, MA). Her spouse Dr. Markus Frank serves as a scientific advisor to Ticeba GmbH and Rheacell GmbH & Co. KG.

Dr. Krier reports no disclosures.

Dr. Gaudet reports no disclosures.

Dr. Gupta was supported by K01 AR062601 (VAG) and the Eleanor and Miles Shore Fellowship for Scholars in Medicine and Brigham and Women's Hospital Career Development Award (VAG).

Word count for abstract: 221

Word count for text: 3218

Abstract

Objective

Hereditary neuropathies form a group of genetic disorders with a broad range of phenotypes, mode of inheritance and causative genes. The objective of this study is to identify the genetic cause of disease in a congenital form of distal hereditary motor neuropathy (dHMN).

Methods

A 2-year-old boy was diagnosed with arthrogryposis multiplex congenital, severe skeletal abnormalities, torticollis, vocal cord paralysis and diminished lower limb movement. Whole exome sequencing was performed on the proband and family members. Structure modeling and functional studies were performed to validate pathogenicity of the identified variant.

Results

Whole exome sequencing revealed a biallelic homozygous mutation in the *TRPV4* gene (c.281C>T; p.S94L). The identification of a novel recessive mutation in *TRPV4* extends the spectrum of mutations in recessive forms of the *TRPV4*-associated disease. Structural modeling and functional studies were performed on p.S94L and other previously identified TRPV4 variants in different protein domains. Structural modeling suggests that the p.S94L mutation is in the disordered N-terminal region proximal to important regulatory binding sites for phosphoinositides and for PACSIN3, which could lead to alternations in trafficking and/or channel sensitivity. Functional studies show that p.S94L reduces TRPV4 protein stability and therefore involves a loss-of-function mechanism.

Conclusion

This study identifies a novel biallelic mutation in *TRPV4* as a cause of the recessive form of congenital form of distal hereditary motor neuropathy (dHMN).

Glossary

dHMN = distal hereditary motor neuropathy; HMSN = hereditary motor and sensory neuropathy; HSAN = hereditary sensory and autonomic neuropathy; SPSMA = scapuloperoneal spinal muscular atrophy; CSMAA = congenital spinal muscular atrophy and arthrogryposis; CMT = Charcot-Marie-Tooth diseases; PBD = phosphoinositide-binding domain; PRR = proline-rich region; PIP2 = phosphatidylinositol biphosphate; FDAB = Familial digital arthropathy-brachydactyly

Hereditary neuropathies are a clinically and genetically heterogeneous group of diseases with an estimated prevalence of 1:2500. Clinical manifestations of hereditary neuropathies include slow progressive distal weakness and muscle wasting with or without sensory loss. Hereditary neuropathies are classified in to three broad categories on the basis of clinical phenotype. Charcot-Marie-Tooth disease or hereditary motor and sensory neuropathy (HMSN) typically exhibits involvement of both motor and sensory systems, hereditary sensory and autonomic neuropathy (HSAN) involves sensory deficits and/or autonomic dysfunction, and distal hereditary neuropathy (dHMN) predominately involves motor deficits. These groups can be further classified into many subtypes depending on electrophysiological criteria, pathological defects, mode of inheritance and molecular genetic defects. These diseases are genetically highly heterogeneous with mutations in at least 80 different genes associated with these subtypes[1, 2]. Despite this significant progress, 30-70% of people affected with neuropathies do not have a genetic diagnosis due to clinical and genetic heterogeneity. Some of disease symptoms can be controlled with generic drugs. However, the identification of the underlying genetic lesion is necessary for accurate disease prognosis, management and family planning, and may ultimately lead to personalized treatments.

Mutations in the *TRPV4* (transient receptor potential vanilloid 4) cation channel gene are a rare cause of dominant inherited axonal neuropathies and skeletal dysplasias [3, 4]. *TRPV4* mutations underlie a wide spectrum of clinical presentation and are associated with distal hereditary neuropathy (dHMN), scapuloperoneal spinal muscular atrophy

(SPSMA), congenital spinal muscular atrophy and arthrogryposis (CSMAA), and autosomal dominant axonal Charcot-Marie-Tooth type 2 (CMT) disease. *TRPV4*-related neuropathies are frequently associated with vocal cord paralysis and occasionally with sensorineural hearing loss. *TRPV4* mutations can also result in autosomal dominant skeletal dysplasias. Typically, different mutations in *TRPV4* gene are associated either neuropathies or skeletal dysplasia; however, some patients exhibit both clinical phenotypes. So far, >20 different mutations in *TRPV4* have been identified in patients with neuropathies. However, functional validation of pathogenicity for many of these variants is still lacking, thus preventing a conclusive genetic diagnosis in these patients. To improve the genetic diagnosis of patients affected with neuropathies, we are using whole exome sequencing (WES) combined with functional validation studies to establish the pathogenicity of variants identified by WES. This work has identified the first *TRPV4* homozygous mutation in a patient presented with congenital spinal muscular atrophy and arthrogryposis. Follow-up functional studies reveal distinct disease mechanisms for different TRPV4 variants and provide novel insights that may inform future therapeutic strategies for these patients.

Results

Clinical Presentation

The male proband was born to unrelated healthy parents of Puerto Rican decent after 37 weeks of gestation (Fig. 1A). He has a healthy sister. The proband was delivered by Caesarian section due to breech position and arthrogryposis multiplex congenita on ultra-sound. At birth, the proband exhibited a right clubfoot, a left congenital vertical

talus, and bilateral flexion deformities of the knees. In addition to lower extremity skeletal deformities, the proband exhibited torticollis, vocal cord paralysis, hypotonia and mild head lag. At age 2 years, the proband could sit independently and walk on his knees. However, he was unable to stand or walk independently. Except for lower limb movement, the proband has normal speech, fine motor and gross motor skills in his upper limbs, normal hearing and visual development. Electromyography (EMG) revealed a motor axonopathy with coexisting denervation and reinnervation changes.

Whole Exome Sequencing (WES)

Whole exome sequencing was performed on the proband and parents. The presence of a single affected male individual in this family is consistent with autosomal recessive inheritance, X-linked inheritance or with a dominant *de novo* mutation. Therefore, pedigree and population based filtering was performed to identify potentially damaging homozygous, X-linked, compound heterozygous and *de novo* variants. We only considered rare coding and splice variants that have <0.1-1 % allele in general healthy population in the gnomAD database (gnomad.broadinstitute.org) depending on dominant or recessive inheritance mode, that is consistent with the prevalence of the disease. In total, 15 potential genes carried a variant (Supplementary Table 1), that were further prioritized using our knowledge-based and crowdsourcing pipeline recently reviewed in Haghighi et al [5]. The top candidate was a homozygous missense variant in *TRPV4* c.281C>T; (p.S94L). Sanger sequencing confirmed the homozygosity of this variant in proband (BGM0049-1) and heterozygous inheritance from both parents (BGM0049-2, -3) (Fig. 1B). The unaffected sister was found to be homozygous for the

normal variant (not shown). The other 14 variants/genes could be ruled out by having low population constraints, known unrelated disease-associations, unrelated protein functions and lack of expression in relevant tissues (Supplementary Table 1), corroborating the potential causal effect of the *TRPV4* variant. This missense variant is highly conserved in most of the vertebrate species and is localized to N-terminus of the TRPV4 protein (Fig. 1C-D).

Structural Model

A recent cryoelectron microscopy (cryoEM) structure of *Xenopus tropicalis* TRPV4 was used to model the position of p.S94L and other previously described neuropathy-causing TRPV4 mutations (Figure 2)[6]. Consistent with previous proteolysis protection and nuclear magnetic resonance studies the N-terminal region – up to residue 139, thus including p.S94 – was disordered and not modeled in the cryoEM structure. However, p.S94L is located N-terminal to two important regulatory regions: a phosphoinositide-binding domain (PBD; residues 107-111) that interacts with PIP_2[7] and a proline-rich region (PRR; residues 124-130) that interacts with the SH3 domain of PACSIN3[8]. PACSIN3 enhances TRPV4 trafficking to the cellular membrane. PIP_2 binding enhances TRPV4 responses to several stimuli whereas PACSIN3 decreases responses to these same stimuli via an antagonistic interaction between two key regulators that is likely mediated through PACSIN3-mediated structural rearrangements of the PRR[7, 9]. Therefore, our structural modeling suggests that the p.S94L mutation could potentially affect the regulation and/or sensitivity of TRPV4.

Functional Modeling of TRPV4 Variants

Functional studies have shown a gain-of-function mechanism for previously known dominant mutations in *TRPV4*[10]. To validate the pathogenicity of the p.S94L variant, functional studies were performed by analyzing the stability and localization of the mutant protein. To compare the magnitude of the functional deficits, known neuropathy-causing p.R269C and p.R315W TRPV4 mutants were analyzed in parallel. In addition, a mutation p.T701I has been reported as a cause of neuropathy. p.T701I is localized to the transmembrane domain S6 helix (Fig. 2), near the vanilloid-binding site in the homologous ion channel TRPV1.[11] Currently, there are no functional studies establishing the pathogenicity of this variant in human diseases or TRPV4 protein functions. Therefore, we investigated the effect of p.S94L, p.R269C, p.R314W and p.T701I on the stability and subcellular localization of TRPV4. To investigate the effect of different variants on protein stability, TRPV4-WT and mutant constructs were transiently expressed in HEK293T cells and expression was analyzed by western blot. Protein analysis by western blot showed an absence of p.S94L protein as well as reduced levels of p.R269C and p.R315W. In contrast, p.T701I exhibited levels of protein expression similar to those of wild-type TRPV4. To examine the sub-cellular localization of p.S94L and other mutants, immunofluorescence analyses were performed. Wild-type TRPV4 primarily localized to the plasma membrane as has been reported for endogenous TRPV4 protein. p.R269C and p.R315W also exhibited localization to the plasma membrane. Interestingly, the p.T701I mutant protein showed a perinuclear localization pattern, and in contrast to wild-type protein, no protein was

detected on the plasma membrane. Consistent with its lack of expression by western blot, no staining for pS94L was observed by immunostaining.

Discussion

Autosomal dominant mutations in *TRPV4* are associated with diverse clinical presentations including distal hereditary motor neuropathy (dHMN), scapuloperoneal spinal muscular atrophy (SPSMA), congenital spinal muscular atrophy and arthrogryposis (CSMAA), and autosomal dominant axonal Charcot-Marie-Tooth type 2 (CMT2) disease. *TRPV4* mutations also result in several forms of autosomal dominant skeletal dysplasias. Several functional studies have demonstrated a gain-of-function mechanism for mutant TRPV4-mediated neuropathies[10]. Mutant TRPV4 proteins frequently exhibit normal localization; however, they demonstrate increased calcium channel activity at both basal and activated levels. This results in increased intracellular calcium concentration leading to cytotoxicity.

Following a combination of whole exome sequencing and functional analysis, we identified a biallelic missense variant, p.S94L, in TRPV4 as a cause of a severe form of distal hereditary motor neuropathy. This serine residue is highly conserved in mammals and only 6 heterozygous and no homozygous individuals are reported in a control population of 246210 people (Genome Aggregation Database, gnomAD), implicating this as a crucial amino acid. Here, we demonstrate that TRPV4 p.S94L severely affects protein stability, thereby impairing TRPV4 localization to the plasma membrane, and consequently its function. This is the first report of loss-of-function in the TRPV4 cation

channel as a cause of disease in a human patient. Previous work has identified reduced stability of many dominant variants in the intracellular ankyrin-repeat domain of TRPV4[12]. A recent study also identified biallelic heterozygous mutations located in the C-terminus of the TRPV4 channel in two siblings with neuropathy associated with severe intellectual disability[13]. These mutant proteins demonstrated normal membrane localization; however, they showed reduced channel function. In contrast, the p.S94L variant resulted in a complete absence of the mutant protein and hence an elimination of TRPV4 channel activity leading to a severe phenotype in the proband.

Interestingly, *Trpv4* knockout mice are viable and fertile, but exhibit an increased bladder capacity due to an impaired stretch sensor in the bladder wall, thicker bones due to impaired osteoclast differentiation, reduced water intake due to altered osmosensation, compromised vascular endothelial function and some sensory defects, such as hearing alteration, impaired sensation and compromised pain sensing. As mammalian genomes contain six *TRPV* genes, a lack of severity of phenotype in mice knockout models could be due to functional redundancy of these channels in mice. The p.S94L mutation is located in the N-terminal intracellular region upstream of the ankyrin repeat domains. Previous studies have shown that dominant mutations in this region result in neuropathy in affected individuals. However, the proband's parents who are heterozygous for the *TRPV4* p.S94L variant did not exhibit any phenotype, as well as 6 heterozygous individuals are reported in the gnomAD database. This could be due to reduced channel function as opposed to the gain-of-function mechanism believed to underlie other *TRPV4* mutations. Nonetheless, many *TRPV4* variants exhibit reduced

penetrance in adult carriers and for this reason, the parents of the proband were counseled to routine follow up in neurology clinic. Interestingly, most human disease-causing variants studied in this work exhibited a reduced protein stability, whereas the p.T701I variant altered the cellular localization of TRPV4 protein, from plasma membrane to the perinuclear area. This mis-localization may result in altered calcium channel function in affected patients. Together, these results demonstrate that different mutations in *TRPV4* affect the channel function by different mechanisms. Understanding the functional alterations in mutant TRPV4 channels is essential not only for determining the pathogenicity of novel variants, but also for the design of specific therapies as both agonists and antagonists of TRPV4 channels are available.

Materials and Methods

Patient consents and standard protocol approvals

The proband, both parents and the affected sibling were enrolled and informed consent was obtained from participants in accord to an Institutional Review Board approved study at Boston Children's Hospital and Brigham and Women's Hospital.

Whole-exome sequencing

DNA extraction from blood samples was performed by the Research Connection Biobank Core (Boston Children's Hospital) using QIAmp DNA Mini kit (Qiagen). Whole exome sequencing was performed by Yale Genome Center. DNA samples from the proband and parents were sent for whole exome sequencing. Samples were prepared as an Illumina sequencing library and enriched for exomic sequences using the Agilent

V5 Sureselect kit. The captured libraries were sequenced using Illumina HiSeq 2000 Sequencers at Lab Corp. FASTQs generated from exome sequencing were filtered and aligned, and variants were filtered and annotated, as previously described[5]. In short, first we apply agnostic filtering, and we use pedigree based inheritance mode filtering for *de novo* , and recessive variants, as well as filter for rare variants only based on large population databases (gnomAD, gnomad.broadinstitute.org). In the second step, we apply several knowledge-based filters on the genes (e.g. known functional and disease associations, expression level data, model organism data) and on the variants (e.g. evolutionary conservation, structural constraints etc.). Finally, the variants were prioritized during a crowdsourcing case conference of interdisciplinary audience.[5]
To validate the *TRPV4* variant, PCR products for the proband, unaffected sibling and parents were analyzed by standard Sanger sequencing (Dana-Farber/Harvard Cancer Center DNA Sequencing Facility).

In silico modeling of TRPV4 mutations

TRPV4 mutations were mapped onto the cryoEM structure of *Xenopus tropicalis* TRPV4 (PDB ID: 6bjj)[6] after aligning the XtTRPV4 and human TRPV4 sequences using Clustal Omega. Figure 2 was generated using PyMOL (Schrodinger).

Cloning of mutant constructs

To generate *TRPV4* mutant plasmids, p.S94L, p.R315W and & p.T701I variants were incorporated into *TRPV4* cDNA using Q5 site-directed mutagenesis kit (New England Biolabs). The mutagenesis primer sequences were: S94L forward: 5'-TAT GAG TCC

TTG GTG GTG CCT-3', S94L reverse: 5'-TAG GGT GGA CTC CAG CAG-3', R315W forward: 5'-GGC GGA CAT GTG GCG CCA GGA-3', R315W reverse: 5'-TTC TTG TGG GGG TTC TCC GTC AGGT-3', T701I forward: 5'-CTG CTG GTG ATC TAC ATC ATC-3', T701I reverse: 5'-GAT GAT GAA GAC CAC GGG-3'.

Cell Culture and Transfection

Human HEK293T cells were cultured in growth medium consisting of DMEM supplemented with 10% fetal bovine serum. Cells were transfected with plasmid DNAs, including control empty vector, using Lipofectamine 3000 (Life Technologies) and harvested after 48 hours for RNA and protein isolation.

Western Blot and Immunofluorescence Analysis

Forty-eight hours after transfection, cell lysates were prepared in RIPA buffer (Thermofisher Scientific) and western blot were performed according to standard protocols. M2 anti-Flag antibody (Sigma F1804, 1:1000) was used to detect TRPV4-tagged proteins. GAPDH (Abcam 8254, 1:10,000) was used as a loading control. Densitometric analysis was performed with imageJ (https://imagej.nih.gov/ij/)

For immunofluorescence, HEK293T cells were plated in 8-chambered slides and transfections were performed as described above. Twenty-four hours after transfection, cells were fixed in 4% paraformaldehyde and immunofluorescence was performed as described previously[14]. M2 anti-Flag antibody (Sigma, 1:250) and sodium potassium

ATPase antibody (Abcam 76020,1:100). Nuclear staining was done using DAPI (Biolegend, 422801).

Data Availability

The research material supporting this publication can be accessed by contacting the corresponding author at “vgupta@research.bwh.harvard.edu”.

Acknowledgement

This work was supported by K01 AR062601 (VAG) and the Eleanor, Miles Shore Fellowship for Scholars in Medicine and Brigham and Women’s Hospital Career Development Award (VAG), a Brigham Biomedical Research Institute Director’s Transformative Award (Brigham Genomic Medicine), and the American Heart Association 16GRNT27250119 (RG).

Appendix I

Name	Location	Role	Contribution
Michael M Marchetti, BS	Brigham and Women's Hospital	Author	Major role in the acquisition of data
Agnes Toth-Petroczy,PhD	Brigham and Women's Hospital	Author	Interpreted the data; revised the manuscript for intellectual content
Claire Grogogeat	Brigham and Women's Hospital	Author	Major role in the acquisition of data
Jose Velilla. BS	Harvard University	Author	Major role in the acquisition of data
Alexis H. Bennett, MS	Brigham and Women's Hospital	Author	Major role in the acquisition of data
Nikkola Carmichael, MS	Brigham and Women's Hospital	Author	Interpreted the data; revised the manuscript for intellectual content
Elicia Estrella, MS	Boston Children's Hospital	Author	Design and conceptualized study; analyzed the data; drafted the manuscript for intellectual content
Basil T. Darras, MD	Boston Children's Hospital	Author	Design and conceptualized study; analyzed the data; drafted the manuscript for intellectual content
Natasha Y. Frank, MD	Brigham and Women's Hospital	Author	Interpreted the data; revised the manuscript for intellectual content
Joel Krier, MD	Brigham and Women's Hospital	Author	Interpreted the data; revised the manuscript for intellectual content
Rachelle Gaudet, PhD	Harvard University	Author	Design and conceptualized study; Interpreted the data; revised the manuscript for intellectual content
Vandana A. Gupta, PhD	Brigham and Women's Hospital	Author	Design and conceptualized study; analyzed the data; drafted the manuscript for intellectual content

References

1. Rossor AM, Polke JM, Houlden H, Reilly MM. Clinical implications of genetic advances in Charcot-Marie-Tooth disease. Nat Rev Neurol 2013;9:562-571.

2. Pareyson D, Saveri P, Pisciotta C. New developments in Charcot-Marie-Tooth neuropathy and related diseases. Curr Opin Neurol 2017;30:471-480.

3. Landoure G, Zdebik AA, Martinez TL, et al. Mutations in TRPV4 cause Charcot-Marie-Tooth disease type 2C. Nat Genet 2010;42:170-174.

4. Rock MJ, Prenen J, Funari VA, et al. Gain-of-function mutations in TRPV4 cause autosomal dominant brachyolmia. Nat Genet 2008;40:999-1003.

5. Haghighi A, Cassa CA, Krier JB, et al. An Integrated Clinical Program and Crowdsourcing Strategy for Genomic Sequencing
and Mendelian Disease Gene Discovery. Genomic Medicine 2018.

6. Deng Z, Paknejad N, Maksaev G, et al. Cryo-EM and X-ray structures of TRPV4 reveal insight into ion permeation and gating mechanisms. Nat Struct Mol Biol 2018;25:252-260.

7. Garcia-Elias A, Mrkonjic S, Pardo-Pastor C, et al. Phosphatidylinositol-4,5-biphosphate-dependent rearrangement of TRPV4 cytosolic tails enables channel activation by physiological stimuli. Proc Natl Acad Sci U S A 2013;110:9553-9558.

8. Cuajungco MP, Grimm C, Oshima K, et al. PACSINs bind to the TRPV4 cation channel. PACSIN 3 modulates the subcellular localization of TRPV4. J Biol Chem 2006;281:18753-18762.

9. D'Hoedt D, Owsianik G, Prenen J, et al. Stimulus-specific modulation of the cation channel TRPV4 by PACSIN 3. J Biol Chem 2008;283:6272-6280.

10. Fecto F, Shi Y, Huda R, Martina M, Siddique T, Deng HX. Mutant TRPV4-mediated toxicity is linked to increased constitutive function in axonal neuropathies. J Biol Chem 2011;286:17281-17291.

11. Gao Y, Cao E, Julius D, Cheng Y. TRPV1 structures in nanodiscs reveal mechanisms of ligand and lipid action. Nature 2016;534:347-351.

12. Inada H, Procko E, Sotomayor M, Gaudet R. Structural and biochemical consequences of disease-causing mutations in the ankyrin repeat domain of the human TRPV4 channel. Biochemistry 2012;51:6195-6206.

13. Thibodeau ML, Peters CH, Townsend KN, et al. Compound heterozygous TRPV4 mutations in two siblings with a complex phenotype including severe intellectual disability and neuropathy. Am J Med Genet A 2017;173:3087-3092.

14. Bennett AH, O'Donohue MF, Gundry SR, et al. RNA helicase, DDX27 regulates skeletal muscle growth and regeneration by modulation of translational processes. PLoS Genet 2018;14:e1007226.

Figure Legends:

Figure 1. (A) Pedigree of family of affected patient; proband is indicated by the arrow (B) Sanger sequencing pherograms show homozygosity for c.281C>T in *TRPV4* in the proband and heterozygosity in both parents. (C) Protein sequence alignment of TRPV4 orthologs showing conservation in the region including p.S94L in higher vertebrates. (D) Schematic diagram of the TRPV4 protein demonstrating localization of p.S94L on the N-terminal intercellular region. Numbers 1-6 correspond to the six ankyrin repeats.

Figure 2. Structural model based on the cryoEM structure of *Xenopus tropicalis* TRPV4 (PDB ID: 6bjj). The structure, corresponding to residues 140-780 (human numbering) does not include disordered N- and C-terminal regions. The N-terminal region is schematized as a dotted line for each subunit, with the phosphoinositide binding domain (PBD; residues 107-111 in human) and proline-rich region (PRR, residues 124-130) indicated. Residue positions for neuropathy-causing mutations (D62N, P97R, R186Q, R232C/S, R237G/L, R269C/H, R315W, R316C/H, S542Y, T701I) and disease mutations with mixed phenotypes (G78W, A217S, E278K, S542Y, V620Y, T740I) are green and yellow, respectively. Position of p.S94L is indicated in purple.

Figure 3: Western blot from HEK293T lysates transiently expressing TRPV4-Flag, p.S94L-Flag, p.R269C-Flag, p.R315W-Flag, p.T701I or empty vector collected 48 hours after transfections. Protein lysates were probed with antibodies against Flag tag to detect transfected wild-type and mutant TRPV4 proteins, and GAPDH as the loading control.

Figure 4: Representative images of HEK293T cells transiently expressing TRPV4-Flag, p.S94L-Flag, p.R269C-Flag, p.R315W-Flag, p.T701I proteins. Immunofluorescence was performed with anti-Flag tag antibody to detect TRPV4-Flag proteins and Na-K-ATPase to label the plasma membrane. Nuclei were stained with DAPI. Scale bar = 20μM.

Figure 1

A

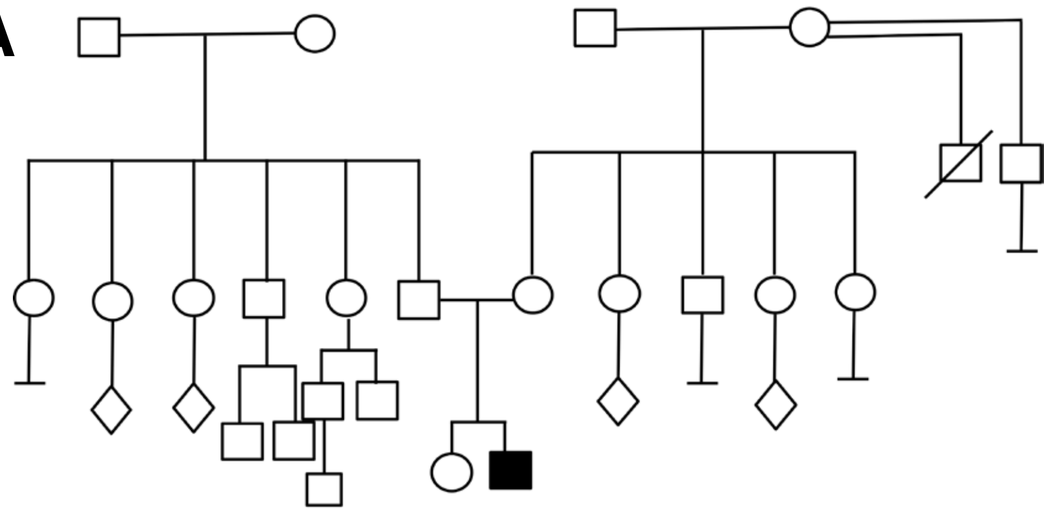

B

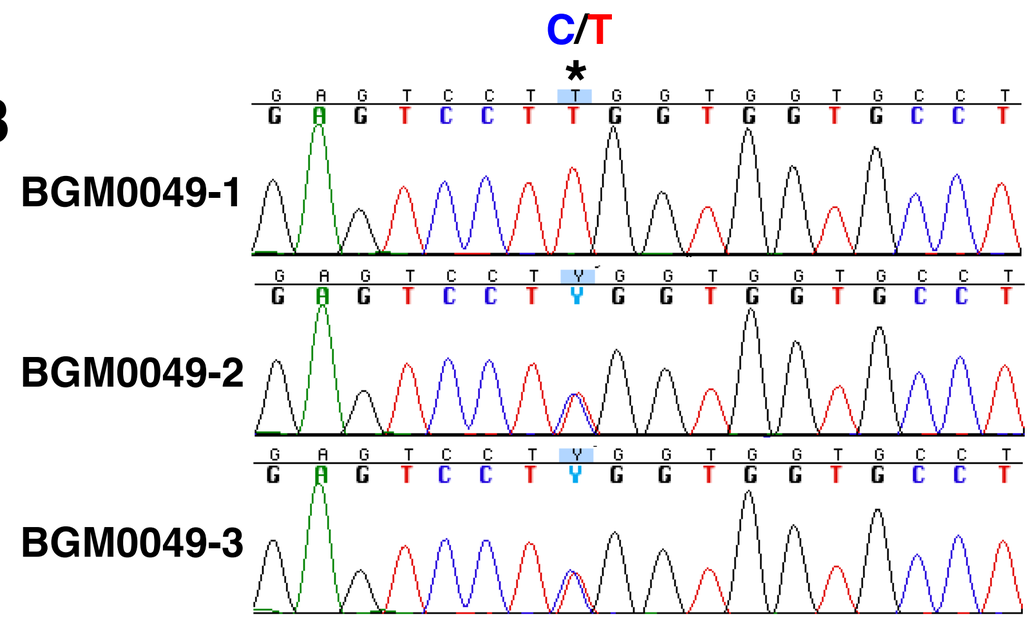

C

Homo sapiens	LESTLYESSVVPGPK
Mus musculus	LESTLYESSVVPGPK
Gallus gallus	LESTIYESSVVPAPK
Xenopus tropicalis	LESTIYESS - - -APK
Takifugu rubripes	LESTIYESNVVPGPK
Danio rerio	LESDY- - - - - TEYPK

D

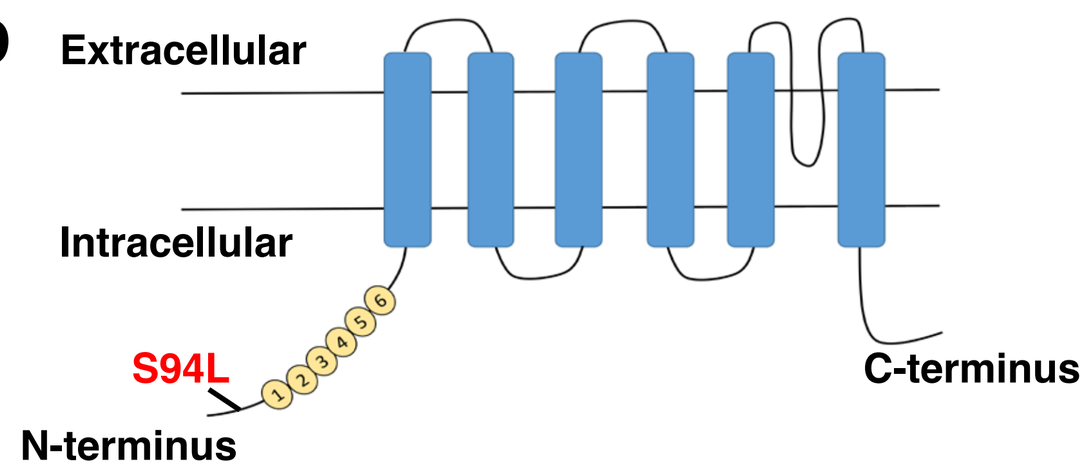

Figure 2

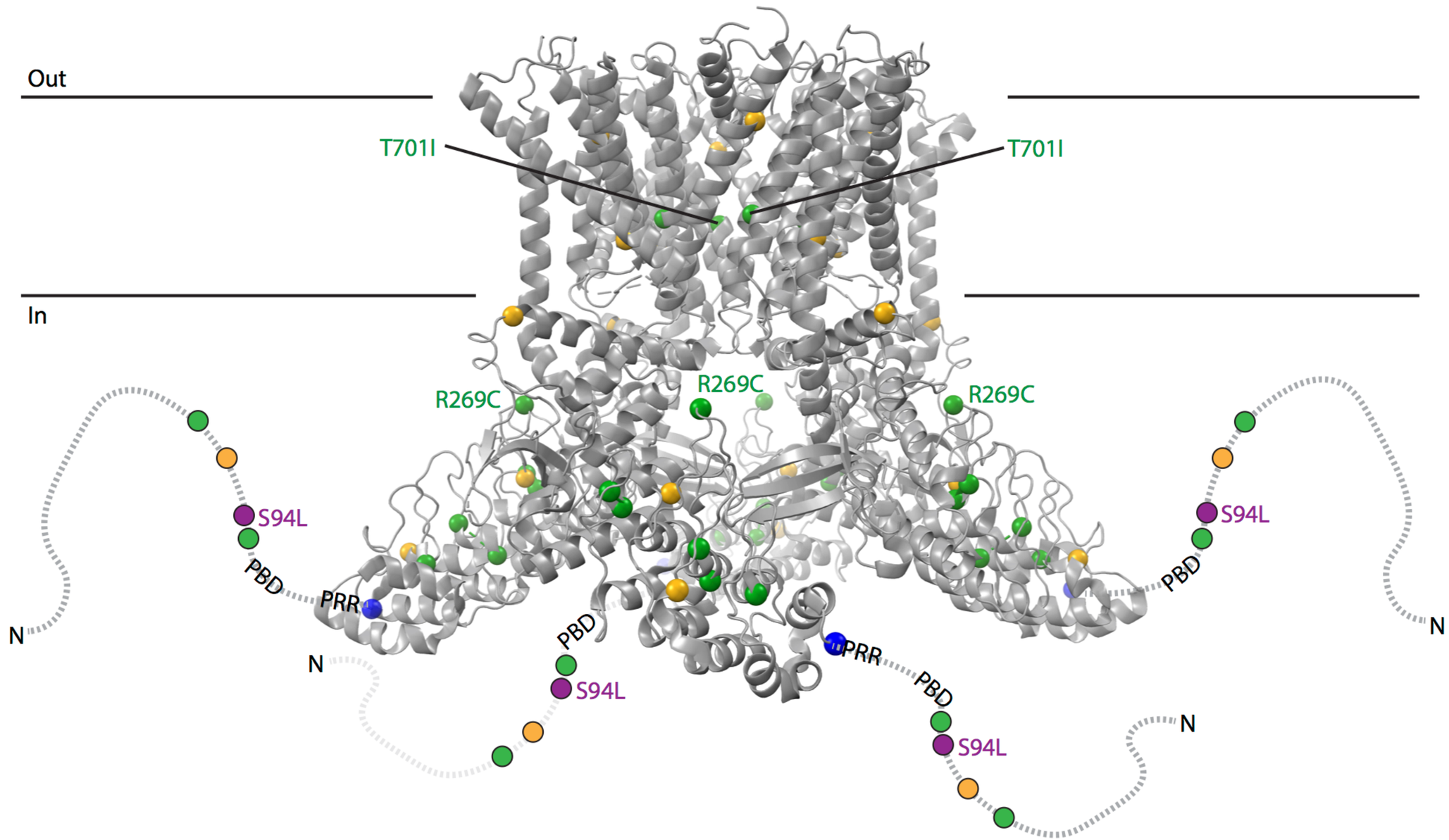
Out
In
T701I
T701I
R269C
R269C
R269C
S94L
S94L
S94L
S94L
PBD
PBD
PBD
PBD
PRR
PRR
N
N
N
N

Figure 3

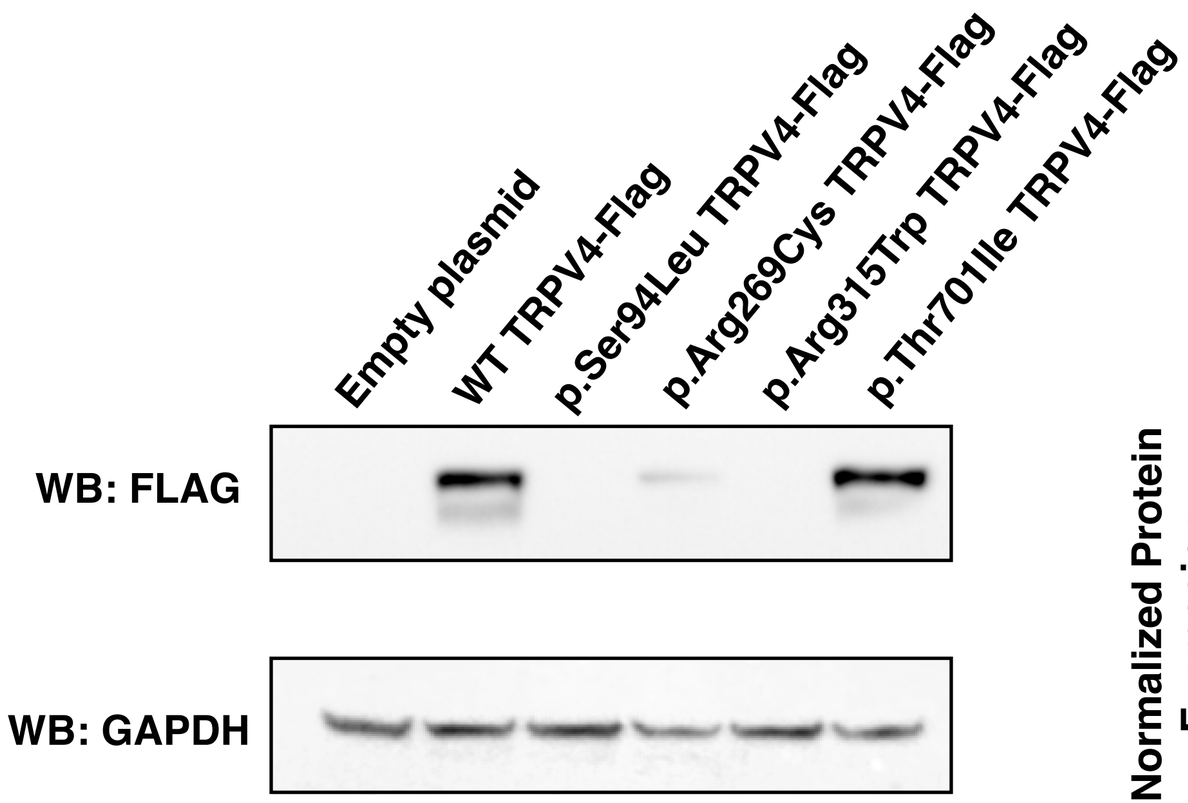
Empty plasmid
WT TRPV4-Flag
p.Ser94Leu TRPV4-Flag
p.Arg269Cys TRPV4-Flag
p.Arg315Trp TRPV4-Flag
p.Thr701Ile TRPV4-Flag
WB: FLAG
WB: GAPDH

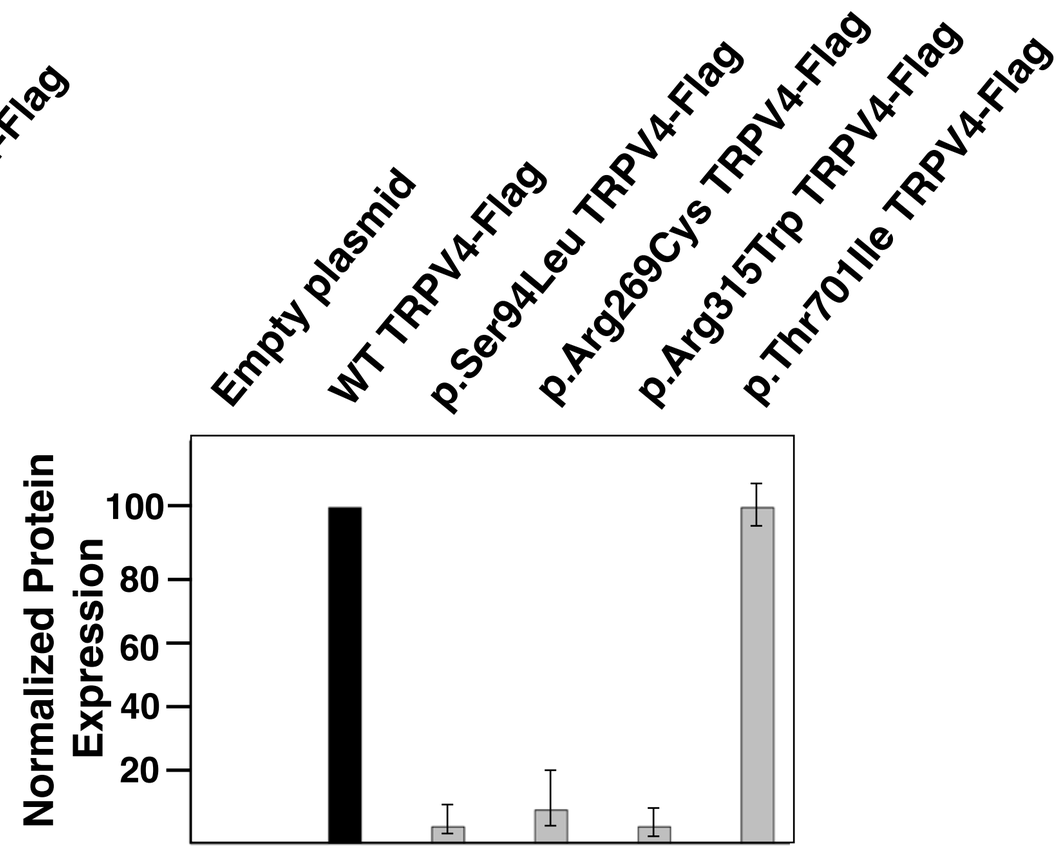
Empty plasmid
WT TRPV4-Flag
p.Ser94Leu TRPV4-Flag
p.Arg269Cys TRPV4-Flag
p.Arg315Trp TRPV4-Flag
p.Thr701Ile TRPV4-Flag
Normalized Protein Expression
100
80
60
40
20

Figure 4

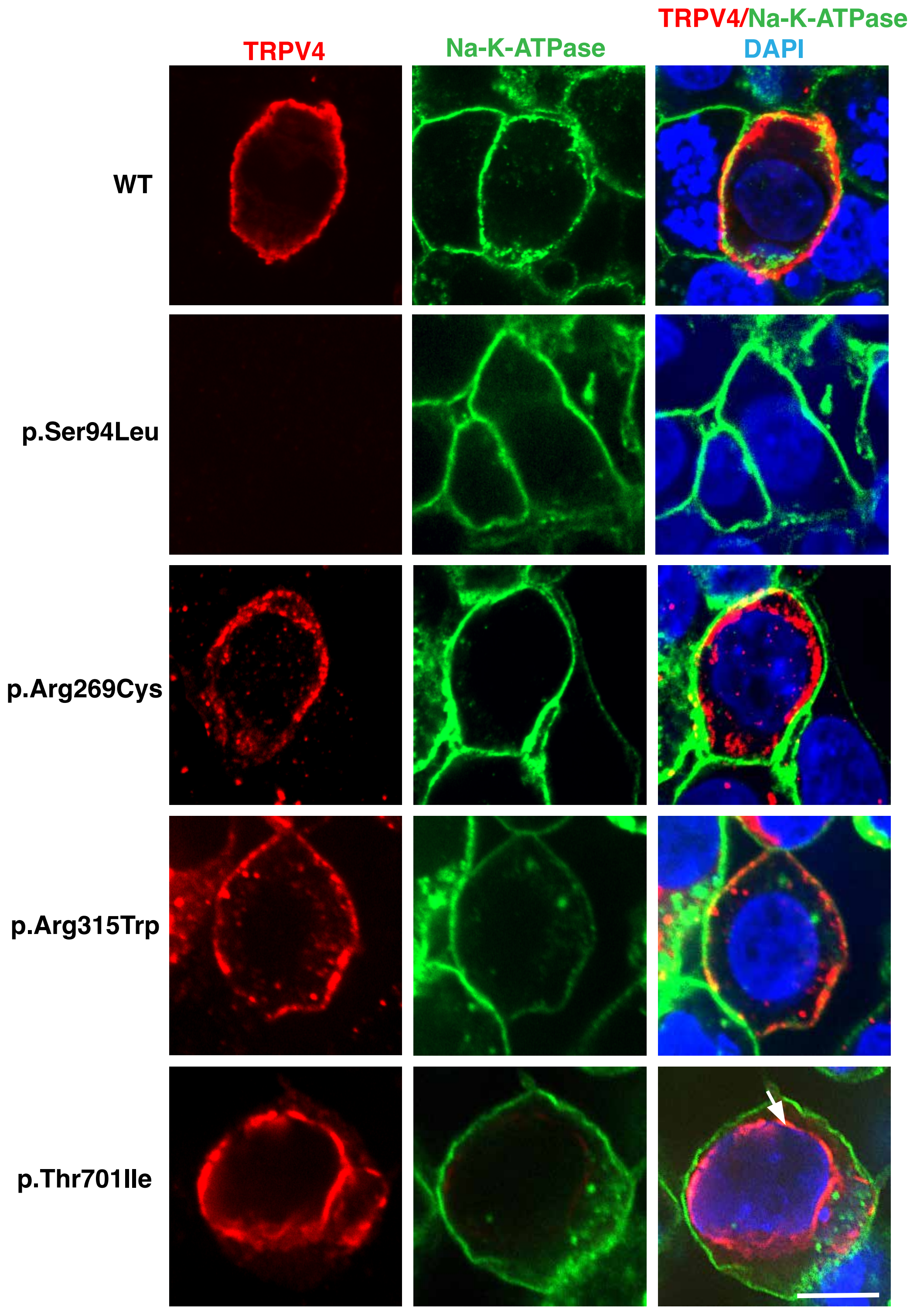
TRPV4
Na-K-ATPase
TRPV4/Na-K-ATPase
DAPI
WT
p.Ser94Leu
p.Arg269Cys
p.Arg315Trp
p.Thr701Ile